One Health 15 (2022) 100462

Contents lists available at ScienceDirect

One Health

journal homepage: www.elsevier.com/locate/onehlt

Modelling the West Nile virus force of infection in the European human population

Giovanni Marini [a,*], Andrea Pugliese [b], William Wint [c], Neil S. Alexander [c], Annapaola Rizzoli [a], Roberto Rosà [a,d]

[a] Research and Innovation Centre, Fondazione Edmund Mach, San Michele all'Adige (TN), Italy
[b] Department of Mathematics, University of Trento, Trento, Italy
[c] Environmental Research Group Oxford, c/o Department of Zoology, Mansfield Road, Oxford, UK
[d] Center Agriculture Food Environment, University of Trento, San Michele all'Adige (TN), Italy

ARTICLE INFO

Keywords:
Mosquito
Vector-borne disease
Mathematical model
Public health

ABSTRACT

West Nile virus (WNV) is among the most recent emerging mosquito-borne pathogens in Europe where each year hundreds of human cases are recorded. We developed a relatively simple technique to model the WNV force of infection (FOI) in the human population to assess its dependence on environmental and human demographic factors. To this aim, we collated WNV human case-based data reported to the European Surveillance System from 15 European Countries during the period 2010–2021. We modelled the regional WNV FOI for each year through normal distributions and calibrated the constituent parameters, namely average (peak timing), variance and overall intensity, to observed cases. Finally, we investigated through regression models how these parameters are associated to a set of climatic, environmental and human demographic covariates. Our modelling approach shows good agreement between expected and observed epidemiological curves. We found that FOI magnitude is positively associated with spring temperature and larger in more anthropogenic semi-natural areas, while FOI peak timing is negatively related to summer temperature. Unsurprisingly, FOI is estimated to be greater in regions with a larger fraction of elderly people, who are more likely to contract severe infections. Our results confirm that temperature plays a key role in shaping WNV transmission in Europe and provide some interesting hints on how human presence and demography might affect WNV burden. This simple yet reliable approach could be easily adopted for early warning and to address epidemiological investigations of other vector-borne diseases, especially where eco-epidemiological data are scarce.

1. Introduction

West Nile Virus (WNV), a flavivirus that was first isolated in Uganda in 1937 [1], is one of the most recent and frequent emerging mosquito-borne pathogens in Europe. WNV is maintained in an enzootic cycle, transmitted primarily between avian hosts and mosquito vectors [2]. Mosquitoes acquire infection after biting an infectious bird and, after an incubation period, they become infectious and thus can transmit the virus through subsequent blood meals. Mammals, including humans and equines, act as incidental hosts in the natural transmission cycle, i.e. they cannot transmit the virus to mosquitoes [2]. However, human to human transmission may occur through blood or organ transplantation. While most human infections are asymptomatic, about 25% of the infections present symptoms such as fever and headache and less than 1% develop more severe neurological complications which can have a fatal outcome [2]. In horses, neurological symptoms are observed in about 8% of the infections, with a fatality rate ranging between 22% and 44% [3]. Several vaccines have been licensed for equids [3] but so far none for humans, for which reducing exposure to mosquito bites remains the most efficient prevention strategy.

WNV (lineage 2) has most probably first arrived in Europe in Hungary thanks to migratory birds at the beginning of the 21st century [4], since when it has spread to many European countries causing thousands of human cases. There is substantial heterogeneity in incidence both spatial (i.e. between and within different countries) and temporal (i.e. between different years). Each year the first cases are usually recorded in June and most of the infections occur between July and October [5]. In Europe, *Culex pipiens* mosquitoes appear to be the

* Corresponding author.
E-mail address: giovanni.marini@fmach.it (G. Marini).

https://doi.org/10.1016/j.onehlt.2022.100462
Received 14 July 2022; Received in revised form 17 November 2022; Accepted 17 November 2022
Available online 21 November 2022

major vector for WNV transmission, while several bird species were found susceptible to infection and in particular high prevalences were observed in wild carrion crows, Eurasian blackbirds, Eurasian blackcaps, European robins, and magpies [6].

Being a significant threat for human health, several modelling efforts have been undertaken both in Europe and North America to investigate WNV circulation and help public health authorities identify areas at risk and determine early warning drivers [7–12]. Essentially, models can be categorized in two macro-groups: statistical, which aim at identifying significant associations between some covariates of interest and epidemiological parameters (e.g. [13–18] and dynamical, which are used to study virus circulation by explicitly mimicking the transmission process (e.g. [7,9,12,19]). As WNV is characterized by a quite complex transmission cycle, design of dynamical models is not so straightforward as usually several simplifying assumptions have to be made. For instance, only one host species is generally considered (see however [20,21]), or mosquito population dynamics might not be explicitly modelled, as in [22]. The use of a mechanistic dynamical model is also hindered by the scarcity of available precise quantitative data on vector abundance or the actual prevalence in mosquito and host populations. Collecting such data might be particularly challenging and demanding, especially at a fine temporal and spatial scale [23]. In this study, we present a simple modelling approach to estimate the WNV force of infection (FOI) in the human population using time series of reported cases only, without any need for additional entomological or avian data. We then carried out a statistical analysis to investigate how WNV FOI is associated with several climatic, environmental and human demographic factors of interest.

2. Materials and methods

2.1. Data collection

We obtained WNV case-based data collected between 2010 and 2021 from The European Surveillance System (TESSy) provided by Austria, Bulgaria, Croatia, Cyprus, Czech Republic, France, Germany, Greece, Hungary, Italy, the Netherlands, Romania, Slovenia, Slovakia, and Spain and released by ECDC. Each WNV notification includes date of disease onset, importation status, age group and the probable place of infection (when available) provided at the NUTS (Nomenclature of territorial units for statistics) 3 level [24]. We restricted our analysis to probable and confirmed autochthonous cases only when the region of infection was identified. We denote by $h_{y,i}(w)$ the number of recorded WNV cases with region i as place of infection with symptoms onset occurred during week w of year y ($w \in \{1, \ldots, 52\}$, $y \in \{2010, \ldots, 2021\}$), by $H_{y,i}$ the whole time series, i.e. $H_{y,i} = \bigcup_{w=1}^{52} h_{y,i}(w)$, and by $\Sigma_{y,i}$ the total number of cases with place of infection identified as i recorded during year y, i.e. $\Sigma_{y,i} = \sum_{w=1}^{52} h_{y,i}(w)$.

We collected bioclimatic, environmental and demographic data from various sources to extract potentially relevant drivers of WNV across the European continent. Monthly 5 km resolution Land Surface Temperature (LST) was derived from the MODIS MOD11c3 datasets [25]. Monthly 5 km resolution cumulative precipitation data were derived from downscaled daily ECMWF ERA5-Land datasets and downloaded from the Climate Data Store [26]. Proportions of land cover classes for each spatial unit were derived from the 2018 Corine Land Cover (CLC) data inventory [27]. The number of inhabitants, also stratified by age group, for each considered NUTS3 region was retrieved from the Eurostat database [28].

2.2. Modelling analysis

We assumed $h_{y,i}(w)$ coming from a Poisson distribution with average $\sum_{t \in T_w} N_i \cdot \lambda_{y,i}(t)$, where $\lambda_{y,i}(t)$ denotes the WNV FOI in region i and year y at day t, T_W represents the set of days in week w and N_i is the number of inhabitants of the region. In addition, we assumed that the FOI for region i and year y could be modelled through the density function of a normal distribution, i.e.

$$\lambda_{y,i}(t) = c_{y,i} \cdot \frac{1}{\sigma_{y,i}\sqrt{2\pi}} e^{-\frac{1}{2}\left(\frac{t-\mu_{y,i}}{\sigma_{y,i}}\right)^2}.$$

Where $\mu_{y,i}$ and $\sigma_{y,i}$ represent respectively the average and standard deviation of the distribution and $c_{y,i}$ is a magnitude rescaling factor, representing the overall intensity of infections in that year and geographical area. These three parameters were estimated by matching the generated epidemiological curve to the observed data through a maximum likelihood approach. Specifically, we computed the Poisson likelihood of observing $H_{y,i}$ (considering only series with $\Sigma_{y,i} \geq 5$) with the set of parameters $\Psi = \{\mu_{y,i}, \sigma_{y,i}, c_{y,i}\}$ as

$$L(H_{y,i}, \Psi) = \prod_{w=1}^{52} e^{-\overline{h_{y,i}(w)}} \cdot \frac{\overline{h_{y,i}(w)}^{h_{y,i}(w)}}{h_{y,i}(w)!}$$

Where $\overline{h_{y,i}(w)}$ represents the number of WNV infections expected during week w according to $\lambda_{y,i}$ computed with parameters Ψ. We estimated the three free parameters by maximizing $L(H_{y,i}, \Psi)$ using the Nelder-Mead algorithm [29]. We denote with M, S and C the estimated distributions of $\mu_{y,i}$, $\sigma_{y,i}$ and $c_{y,i}$ respectively. We also carried out a sensitivity analysis (see Appendix A) by modelling $\lambda_{y,i}$ through the density function of a gamma distribution.

We then quantified the relationships between the response variables S, M and C with a set of 7 covariates of potential interest, suggested by previously published studies [8,13,30]:

1) $\eta(i)$: the total percentage of CLC labelled as urban or agricultural area. This measure can be interpreted as a proxy of the anthropogenic impact on the region i.

2–3) $T_{spring}(y,i)$ and $T_{summer}(y,i)$: respectively the average spring (April–May) and summer (June–July) LST recorded in region i during year y.

4–5) $P_{spring}(y,i)$ and $P_{summer}(y,i)$: respectively the cumulated spring (April–May) and summer (June–July) precipitation occured in region i during year y.

6) $\xi(i)$: the fraction of people older than 65 years living in region i.

7) $WNV\_BEFORE_{y,i}$: a factor variable defined as in [30]. Specifically, the factor is set to 0 if no WNV was recorded the previous year; 1 if WNV was recorded the previous year, and NR (not Recorded) for the first year the disease was recorded.

We first computed a full Linear Model which can be represented by the following equation:

$$Y \sim \eta + T_{spring} + T_{summer} + P_{spring} + P_{summer} + \xi + WNV\_BEFORE.$$

Where Y can either be S, M or $\log(C)$ (we normalized the C distribution by log-transforming it). We checked for potential collinearity among explanatory variables by computing Variance Inflation Factors (VIFs) [31]. We then computed all possible submodels and selected as best the model with the lowest Akaike Information Criterion (AIC) score and whose coefficients were all statistically different from 0 at 5% level. Model assumptions were verified by checking residuals distributions and by plotting residuals versus fitted values and versus each covariate in the model [31]. All analysis was carried out in R v4.2.0 [32] using libraries “tidyverse” [33] and “MuMIn” [34].

3. Results

Between 2010 and 2021, a total of 3300 autochthonous cases were reported from 190 different NUTS3 regions located especially in Southern and Eastern Europe (Fig. 1a). The lowest number of infections was observed in 2014 (42 cases), and the highest (1434 cases) in 2018. The cumulative epidemiological curve (total number of cases per week

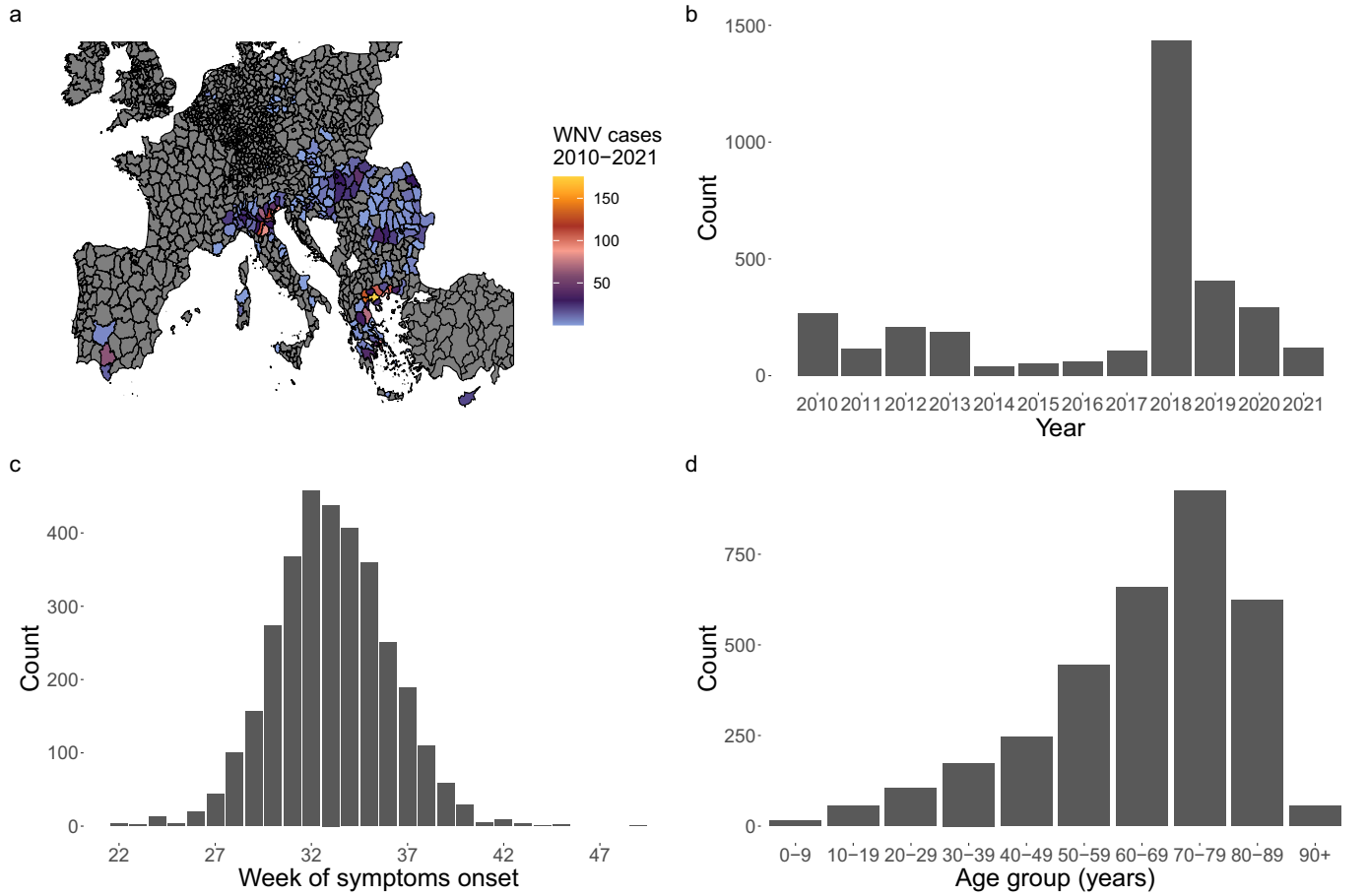

Fig. 1. WNV cases recorded in Europe between 2010 and 2021. Total number of cases by administrative area (NUTS3 level, panel a), by year (panel b), by week of symptoms onset (panel c) and by age group (panel d). Administrative boundaries were retrieved from [24].

of symptoms onset across all years and countries, Fig. 1c) clearly shows a peak around the 32nd week of the year (first half of August). Finally, Fig. 1d highlights the observed higher likelihood for older people to develop symptoms and thus being notified to the surveillance system.

Panels a & b in Fig. 2 show some different realizations for the force of infection λ obtained with different parameter combinations. The timing of the FOI peak depends on the average μ, which indicates the Julian day for which λ reaches its maximum. The curve width can depend on σ: a smaller value corresponds to a steeper curve, if the other two parameters do not change. Thus, σ provides an estimate for the length (in days) of the epidemiological season. Finally, parameter c by definition rescales the whole curve, hence it can be interpreted as a measure of the FOI magnitude. It is thus clear that the total number of expected infections depends directly on c, while σ and μ can be regarded as parameters concerning the timing of infections.

We applied our FOI modelling approach to 172 epidemiological curves $H_{y,i}$ with on average 15.9 total cases (min = 5, max = 96, sd = 15.2). An instance of fit is presented in Fig. 2c, while additional

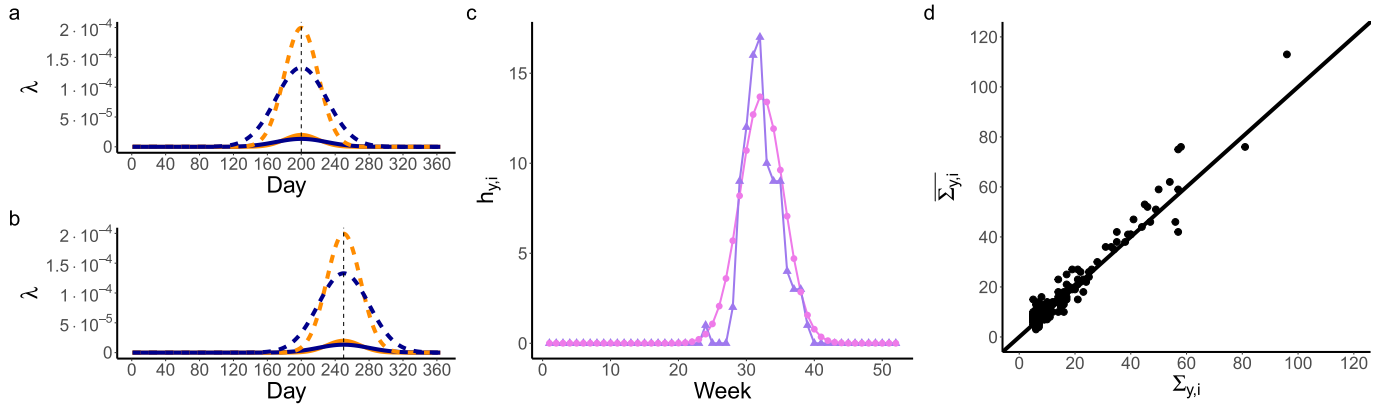

Fig. 2. FOI model. Panels a-b: examples of λ realization with c = 0.01, 0.001 (dashed and continuous lines respectively), σ = 20, 30 (orange and blue respectively) and μ = 200, 250 (panel a and b respectively, shown by the vertical dashed line). Panel c: predicted (pink, circles) and observed (purple, triangles) WNV cases for a selected time series $H_{y,i}$. Panel d: predicted ($\overline{\Sigma_{y,i}}$) and observed ($\Sigma_{y,\,i}$) total yearly number of WNV cases for each region. (For interpretation of the references to colour in this figure legend, the reader is referred to the web version of this article.)

examples can be found in the Appendix A. We can note that qualitatively the modelled time series well matches the observed one. Moreover, we generated stochastically the number of cases with day of symptoms onset t expected for region i and year y by drawing from a Poisson distribution Pois($\lambda_{y,i}(t)$) and found that 99% of the simulated total number of weekly cases lie within the 95% Confidence Interval (CI) of model predictions (see Appendix A). Finally, there is a very good correlation (Pearson correlation coefficient = 0.97) between the predicted and observed $\Sigma_{y,i}$ values (Fig. 2d), with an average squared error $E\left(\Sigma_{y,i} - \overline{\Sigma_{y,i}}\right)^2 = 17.2$. Modelling $\lambda_{y,i}$ through a gamma distribution density function yielded a worse fit (see Appendix A).

Fig. 3 shows the estimated distributions of the three free parameters (c, μ, σ) over all years and geographical areas. The average parameter μ ranged between 195 and 275 (July 16–October 3) with a mean value of 232 (August 21) and a 95%Confidence Interval (CI) lying within 205–256 (July 25–September 14)). The average for S is about 26.5 days (95%CI 10–49.2). Finally, the rescaling parameter is on average $5.94 \bullet 10^{-5}$ (95%CI $5.8 \bullet 10^{-6}$-$3.2 \bullet 10^{-4}$).

We built the full models to statistically investigate how the estimated values of the three parameters are associated with non-collinear covariates of interest as explained in the Methods section. VIFs were all below 3 so we did not discard any explanatory variable [31]. The best model for C, whose coefficients are reported in Table 1, includes three covariates. As shown also in Fig. 4, we found that FOI magnitude is positively associated with spring temperature (T_{spring}) and decreases when human impact on the environment (η) increases. Moreover, FOI is estimated to be greater in areas with higher proportions of elderly people (ξ). The best model for M includes only the average summer temperature (see Table 1) indicating that warmer summers correspond to an earlier timing of the incidence peak. Finally, for S none of covariates was statistically significant.

Table 1
Estimates, standard errors, t values and p-values of the parameters of the best models for C and M.

Y	Parameter	Coefficient Estimate	Standard Error	t value	p-value
C	Intercept	−12.697	0.806	−15.752	<0.001
	η	−0.028	0.004	−7.352	<0.001
	ξ	8.808	1.907	4.618	<0.001
	T_{spring}	0.142	0.036	3.927	<0.001
M	Intercept	258.7	9.592	26.97	<0.001
	T_{summer}	−1.113	0.389	−2.858	0.005

4. Discussion

WNV has becoming an increasing concern for public health authorities in several European countries. Its recent introduction to northern areas in Germany and the Netherlands [35] confirms the potential environmental suitability for its establishment and spread into new as yet unaffected geographic areas in the continent, calling for effective preventive and responsive measures.

Because of its complex cycle, modelling WNV transmission is not so straightforward, especially when detailed quantitative data on mosquito and host abundance along with their infection rates are scarce or not available. Here we proposed a simple yet reliable framework to model the WNV FOI using only human case data, which can also be realized stochastically (see Appendix A). Its simplicity lies in the modelling assumptions, as the incidence is represented by a normal distribution function with three free parameters which can be easily interpreted. Namely, μ measures the timing of the maximum incidence, σ provides an indication for the length of the epidemiological season and c quantifies the overall incidence magnitude. Hence, the infection is implicitly modelled by a Susceptible-Infected-Susceptible (SIS) model [36] with an external FOI. We did not consider an SIR (Recovered) model as recorded human cases are a negligible fraction compared to the total population of the areas under study. Moreover, at the moment, there are no available quantifications of human immunization following infection.

Our analysis highlights different drivers shaping the WNV FOI in Europe. We found that spring temperatures are positively associated with C. This confirms previous findings remarking the importance of spring conditions in Europe for WNV circulation [12,15,30]. Similarly, the timing of the peak WNV incidence appears to be influenced only by summer temperature; infection peak tends to be earlier when summer temperature is higher. Indeed, warmer conditions might amplify virus transmission by increasing the biting rate [37,38] and the host-to-vector transmission probability [39,40] and by accelerating the mosquito viral incubation period [41]. On the other hand, high summer temperatures increase mosquito mortality [42], thus decreasing infection risk. The WNV FOI is expected to be higher in more natural less disturbed habitats, where avian competent hosts might be more likely to dwell or mosquito abundance might be higher [43], and complies with previous findings of a positive association between WNV circulation and presence of anthropized semi-natural areas such as populated forests [15], wetlands [17] and river basins [14]. Finally, FOI is estimated to be greater in areas with a higher number of elderly (age > 65 years) people, consistent with the fact that age is one of the main risk factors for developing severe symptoms upon infection [44].

It is interesting to note that σ, which can be interpreted as a measure of the length of the epidemiological season, has no significant association with any of the considered covariates. However, we found that σ has a significant negative association with the magnitude rescaling factor c (see Appendix A). Indeed, a higher value of c increases the value of λ at all times of a year, and thus the length of the period in which cases are reported. On this basis, we can regard c, which is affected by different abiotic factors, as the most important parameter at shaping the FOI and predicting human incidence. A significant negative association has also been found between M and C, suggesting that in years with a longer period with WNV cases, the infection peak tends to occur earlier.

We found that the model parameters are not significantly associated with precipitation-related variables, possibly because rainfall affects mosquito population dynamics in different ways. On one hand, precipitation can exert a positive influence by creating more breeding sites. On

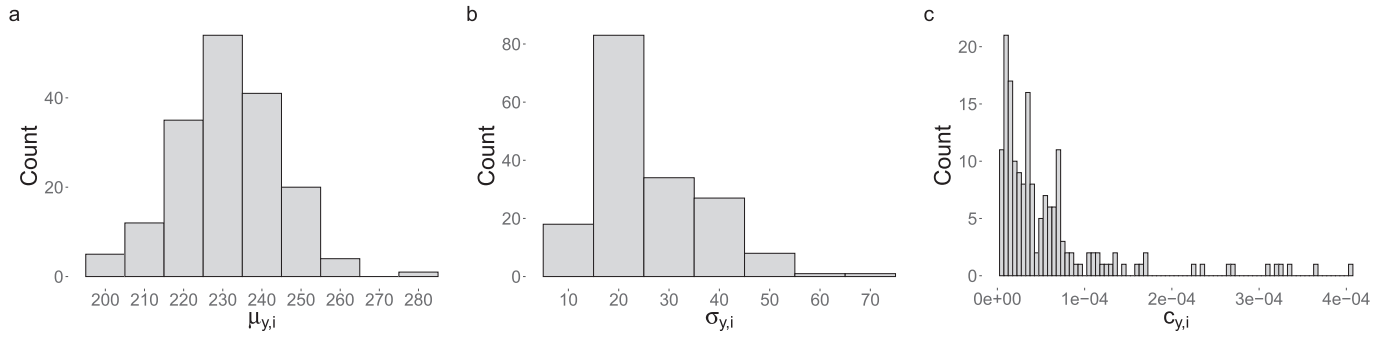

Fig. 3. Estimated M, S and C distributions (panel a-c respectively).

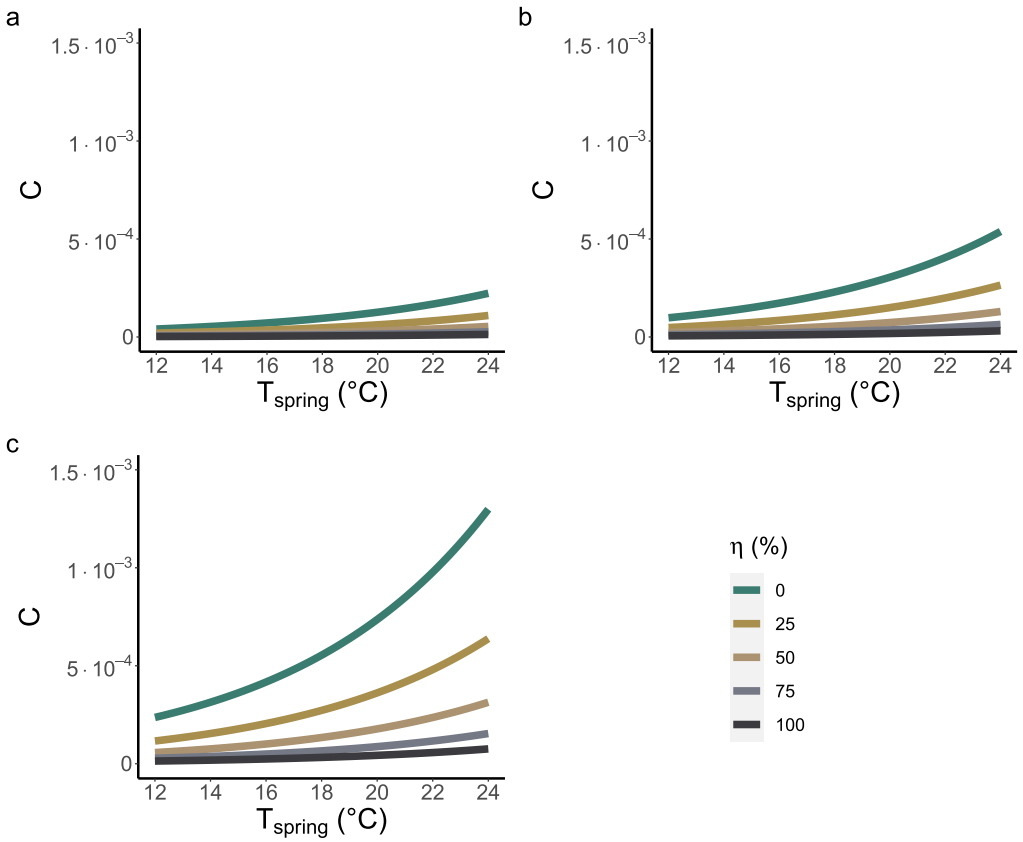

Fig. 4. Best model predictions for *C* according to average spring temperature (x axis) for different levels of human impact (η) and fractions of people older than 65 years (ξ = 0.1, 0.2 and 0.3, panel a-c respectively).

the other hand, heavy rainfall might have a flushing effect on immature populations, eventually decreasing their abundance. Consistently, previous studies reported different associations between precipitation and WNV human incidence in Europe, either negative [45], positive [15] or even inconsistent [16]. Notice that instead [18] found that high humidity in early spring is positively correlated with WNV infections in Texas.

Finally, we found that WNV detection in previous years was not associated with any parameter; this differs from the result found in a previous study in a very similar context (same geographical area and slightly shorter time period) [30]. It has to be noted that in this study we analysed only areas with a high WNV circulation (we applied our modelling approach to (*y*, *i*) such that $\Sigma_{y,\,i} \geq 5$) while in the prior study WNV absence was explicitly considered. The analysis of WNV presence/absence is beyond the scope of the current study but might be included in a future modelling effort.

To the best of our knowledge, this is one of the first attempts at explicitly modelling the WNV FOI in Europe using detailed data on human cases only. If more detailed data, such as entomological collections providing both mosquito abundance and WNV prevalence, are available, then more sophisticated models might be developed to explicitly consider mosquito population dynamics and WNV transmission between vector and host populations, also taking into account temperature-dependent parameters [7,12,22]. However, collecting such data might be very demanding and not always possible, especially at a fine spatial and temporal resolution. Our approach might therefore offer a simple analytical solution as it requires only human data, which are usually routinely collected by European health authorities. The modelling framework might be used to investigate WNV infection dynamics also in wild birds, if avian epidemiological data is available. However, we remark that in this case the FOI function λ should be modified in order to depend also on the current infection rate in the avian population, as birds are competent hosts for the virus. Moreover, birds' mobility should be accounted for, so for instance the FOI in a region could depend also on the ones in the neighbouring areas.

An important outcome of the study is that it confirms the association between unusually high spring temperature and intensity of WNV infection, that was established both through a mechanistic model [12] and by a statistical association with total number of yearly cases [30]. Thus, this association could be tested as a forecasting tool to provide early estimates of the potential burden of WNV on human health later in the season, and possibly target adequate control measures. Finally, we remark that our proposed modelling framework it is not specifically designed for WNV only but it could be applied to any other vector-borne disease for which the FOI has a seasonal pattern and does not depend on the number of infectious humans such as tick-borne encephalitis [46,47] or Usutu [48].

Disclaimer

The views and opinions of the authors expressed herein do not necessarily state or reflect those of ECDC. The accuracy of the authors' statistical analysis and the findings they report are not the responsibility of ECDC. ECDC is not responsible for conclusions or opinions drawn from the data provided. ECDC is not responsible for the correctness of the data and for data management, data merging and data collation after provision of the data. ECDC shall not be held liable for improper or incorrect use of the data.

CRediT authorship contribution statement

Giovanni Marini: Conceptualization, Data curation, Formal analysis, Methodology, Writing – original draft, Writing – review & editing. **Andrea Pugliese:** Conceptualization, Methodology, Writing – review &

editing. **William Wint:** Resources, Writing – review & editing. **Neil S. Alexander:** Resources, Writing – review & editing. **Annapaola Rizzoli:** Writing – review & editing. **Roberto Rosà:** Conceptualization, Methodology, Writing – review & editing.

Declaration of Competing Interest

The authors declare no conflict of interest.

Data availability

The authors do not have permission to share data.

Acknowledgements

This study was partially funded by EU grant 874850 MOOD and is catalogued as MOOD 042. The contents of this publication are the sole responsibility of the authors and don't necessarily reflect the views of the European Commission.

Supplementary data

Supplementary data to this article can be found online at https://doi.org/10.1016/j.onehlt.2022.100462.

References

[1] K.C. Smithburn, T.P. Hughes, A.W. Burke, J.H. Paul, A neurotropic virus isolated from the blood of a native of Uganda, Am. J. Trop. Med. 20 (1940) 471–472.
[2] L.R. Petersen, A.C. Brault, R.S. Nasci, West Nile virus: review of the literature, JAMA. 310 (2013) 308–315, https://doi.org/10.1001/jama.2013.8042.
[3] J. Angenvoort, A.C. Brault, R.A. Bowen, M.H. Groschup, West Nile viral infection of equids, Vet. Microbiol. 167 (2013) 168–180, https://doi.org/10.1016/j.vetmic.2013.08.013.
[4] L.M. Hernández-Triana, C.L. Jeffries, K.L. Mansfield, G. Carnell, A.R. Fooks, N. Johnson, Emergence of West Nile Virus Lineage 2 in Europe: A review on the introduction and spread of a mosquito-borne disease, Front. Public Health 2 (2014), https://doi.org/10.3389/fpubh.2014.00271.
[5] European Centre for Disease Prevention and Control, West Nile virus infection, in: ECDC Annu. Epidemiol. Rep. 2019, ECDC, Stockholm, 2021.
[6] B. Nikolay, A review of West Nile and Usutu virus co-circulation in Europe: how much do transmission cycles overlap? Trans. R. Soc. Trop. Med. Hyg. 109 (2015) 609–618, https://doi.org/10.1093/trstmh/trv066.
[7] S. Bhowmick, J. Gethmann, F.J. Conraths, I.M. Sokolov, H.H.K. Lentz, Locally temperature - driven mathematical model of West Nile virus spread in Germany, J. Theor. Biol. 488 (2020), 110117, https://doi.org/10.1016/j.jtbi.2019.110117.
[8] S. Brugueras, B. Fernández-Martínez, J. Martínez-de la Puente, J. Figuerola, T. M. Porro, C. Rius, A. Larrauri, D. Gómez-Barroso, Environmental drivers, climate change and emergent diseases transmitted by mosquitoes and their vectors in southern Europe: A systematic review, Environ. Res. 191 (2020), 110038, https://doi.org/10.1016/j.envres.2020.110038.
[9] N.B. DeFelice, Z.D. Schneider, E. Little, C. Barker, K.A. Caillouet, S.R. Campbell, D. Damian, P. Irwin, H.M.P. Jones, J. Townsend, J. Shaman, Use of temperature to improve West Nile virus forecasts, PLoS Comput. Biol. 14 (2018), e1006047, https://doi.org/10.1371/journal.pcbi.1006047.
[10] A.C. Keyel, M.E. Gorris, I. Rochlin, J.A. Uelmen, L.F. Chaves, G.L. Hamer, I. K. Moise, M. Shocket, A.M. Kilpatrick, N.B. DeFelice, J.K. Davis, E. Little, P. Irwin, A.J. Tyre, K.H. Smith, C.L. Fredregill, O.E. Timm, K.M. Holcomb, M.C. Wimberly, M.J. Ward, C.M. Barker, C.G. Rhodes, R.L. Smith, A proposed framework for the development and qualitative evaluation of West Nile virus models and their application to local public health decision-making, PLoS Negl. Trop. Dis. 15 (2021), e0009653, https://doi.org/10.1371/journal.pntd.0009653.
[11] I. Kioutsioukis, N.I. Stilianakis, Assessment of West nile virus transmission risk from a weather-dependent epidemiological model and a global sensitivity analysis framework, Acta Trop. 193 (2019) 129–141, https://doi.org/10.1016/j.actatropica.2019.03.003.
[12] G. Marini, M. Calzolari, P. Angelini, R. Bellini, S. Bellini, L. Bolzoni, D. Torri, F. Defilippo, I. Dorigatti, B. Nikolay, A. Pugliese, R. Rosà, M. Tamba, A quantitative comparison of West Nile virus incidence from 2013 to 2018 in Emilia-Romagna, Italy, PLoS Negl. Trop. Dis. 14 (2020), e0007953, https://doi.org/10.1371/journal.pntd.0007953.
[13] Z. Farooq, J. Rocklöv, J. Wallin, N. Abiri, M.O. Sewe, H. Sjödin, J.C. Semenza, Artificial intelligence to predict West Nile virus outbreaks with eco-climatic drivers, Lancet Reg. Health - Eur. 17 (2022), 100370, https://doi.org/10.1016/j.lanepe.2022.100370.
[14] J.-M. García-Carrasco, A.-R. Muñoz, J. Olivero, M. Segura, R. Real, Predicting the spatio-temporal spread of West Nile virus in Europe, PLoS Negl. Trop. Dis. 15 (2021), e0009022, https://doi.org/10.1371/journal.pntd.0009022.
[15] M. Marcantonio, A. Rizzoli, M. Metz, R. Rosà, G. Marini, E. Chadwick, M. Neteler, Identifying the environmental conditions favouring West Nile Virus Outbreaks in Europe, PLoS One 10 (2015), e0121158, https://doi.org/10.1371/journal.pone.0121158.
[16] S. Paz, D. Malkinson, M.S. Green, G. Tsioni, A. Papa, K. Danis, A. Sirbu, C. Ceianu, K. Katalin, E. Ferenczi, H. Zeller, J.C. Semenza, Permissive summer temperatures of the 2010 European West Nile Fever Upsurge, PLoS One 8 (2013), e56398, https://doi.org/10.1371/journal.pone.0056398.
[17] A. Sánchez-Gómez, C. Amela, E. Fernández-Carrión, M. Martínez-Avilés, J. M. Sánchez-Vizcaíno, M.J. Sierra-Moros, Risk mapping of West Nile virus circulation in Spain, 2015, Acta Trop. 169 (2017) 163–169, https://doi.org/10.1016/j.actatropica.2017.02.022.
[18] I. Ukawuba, J. Shaman, Association of spring-summer hydrology and meteorology with human West Nile virus infection in West Texas, USA, 2002–2016, Parasit. Vectors 11 (2018) 224, https://doi.org/10.1186/s13071-018-2781-0.
[19] C. Bowman, A.B. Gumel, P. van den Driessche, J. Wu, H. Zhu, A mathematical model for assessing control strategies against West Nile virus, Bull. Math. Biol. 67 (2005) 1107–1133, https://doi.org/10.1016/j.bulm.2005.01.002.
[20] G. Cruz-Pacheco, L. Esteva, C. Vargas, Multi-species interactions in West Nile virus infection, J. Biol. Dyn. 6 (2012) 281–298, https://doi.org/10.1080/17513758.2011.571721.
[21] J.E. Simpson, P.J. Hurtado, J. Medlock, G. Molaei, T.G. Andreadis, A.P. Galvani, M. A. Diuk-Wasser, Vector host-feeding preferences drive transmission of multi-host pathogens: West Nile virus as a model system, Proc. Biol. Sci. 279 (2012) 925–933, https://doi.org/10.1098/rspb.2011.1282.
[22] G. Marini, R. Rosà, A. Pugliese, A. Rizzoli, C. Rizzo, F. Russo, F. Montarsi, G. Capelli, West Nile virus transmission and human infection risk in Veneto (Italy): a modelling analysis, Sci. Rep. 8 (2018) 14005, https://doi.org/10.1038/s41598-018-32401-6.
[23] B. Caputo, M. Manica, Mosquito surveillance and disease outbreak risk models to inform mosquito-control operations in Europe, Curr. Opin. Insect Sci. 39 (2020) 101–108, https://doi.org/10.1016/j.cois.2020.03.009.
[24] Eurostat, NUTS - GISCO - Eurostat. https://ec.europa.eu/eurostat/web/gisco/geodata/reference-data/administrative-units-statistical-units/nuts, 2022 (accessed May 2, 2022).
[25] Zhengming Wan, Simon Hook, Glynn Hulley, MODIS/Terra Land Surface Temperature/Emissivity Monthly L3 Global 0.05Deg CMG V061, 2021, https://doi.org/10.5067/MODIS/MOD11C3.061.
[26] Copernicus Climate Change Service, ERA5-Land Hourly Data from 2001 to Present, 2019 doi:10.24381/CDS.E2161BAC.
[27] European Environment Agency, CORINE Land Cover — Copernicus Land Monitoring Service. https://land.copernicus.eu/pan-european/corine-land-cover, 2022 (accessed April 29, 2022).
[28] Eurostat, Database. https://ec.europa.eu/eurostat/web/main/data/database, 2022 (accessed April 29, 2022).
[29] J.A. Nelder, R. Mead, A simplex method for function minimization, Comput. J. 7 (1965) 308–313, https://doi.org/10.1093/comjnl/7.4.308.
[30] G. Marini, M. Manica, L. Delucchi, A. Pugliese, R. Rosà, Spring temperature shapes West Nile virus transmission in Europe, Acta Trop. 215 (2021) 105796, https://doi.org/10.1016/j.actatropica.2020.105796.
[31] A.F. Zuur, E.N. Ieno, C.S. Elphick, A protocol for data exploration to avoid common statistical problems, Methods Ecol. Evol. 1 (2010) 3–14, https://doi.org/10.1111/j.2041-210X.2009.00001.x.
[32] R Core Team, R: A Language and Environment for Statistical Computing, R Foundation for Statistical Computing, Vienna, Austria. https://www.R-project.org/, 2022.
[33] H. Wickham, M. Averick, J. Bryan, W. Chang, L. McGowan, R. François, G. Grolemund, A. Hayes, L. Henry, J. Hester, M. Kuhn, T. Pedersen, E. Miller, S. Bache, K. Müller, J. Ooms, D. Robinson, D. Seidel, V. Spinu, K. Takahashi, D. Vaughan, C. Wilke, K. Woo, H. Yutani, Welcome to the Tidyverse, J. Open Source Softw. 4 (2019) 1686, https://doi.org/10.21105/joss.01686.
[34] K. Barton, MuMIn: Multi-Model Inference. https://CRAN.R-project.org/package=MuMIn, 2022.
[35] European Centre for Disease Prevention and Control, Epidemiological update: West Nile virus transmission season in Europe, 2020, Eur. Cent. Dis. Prev. Control. (2021). https://www.ecdc.europa.eu/en/news-events/epidemiological-update-west-nile-virus-transmission-season-europe-2020 (accessed May 2, 2022).
[36] M.J. Keeling, P. Rohani, Modeling Infectious Diseases in Humans and Animals, Princeton University Press, Princeton, 2008.
[37] D.A. Ewing, C.A. Cobbold, B.V. Purse, M.A. Nunn, S.M. White, Modelling the effect of temperature on the seasonal population dynamics of temperate mosquitoes, J. Theor. Biol. 400 (2016) 65–79, https://doi.org/10.1016/j.jtbi.2016.04.008.
[38] J.E. Ruybal, L.D. Kramer, A.M. Kilpatrick, Geographic variation in the response of Culex pipiens life history traits to temperature, Parasit. Vectors 9 (2016) 116, https://doi.org/10.1186/s13071-016-1402-z.
[39] C.M. Holicki, U. Ziegler, C. Răileanu, H. Kampen, D. Werner, J. Schulz, C. Silaghi, M.H. Groschup, A. Vasić, West Nile Virus Lineage 2 vector competence of indigenous culex and aedes mosquitoes from germany at temperate climate conditions, Viruses. 12 (2020) 561, https://doi.org/10.3390/v12050561.
[40] C.B.F. Vogels, J.J. Fros, G.P. Göertz, G.P. Pijlman, C.J.M. Koenraadt, Vector competence of northern European Culex pipiens biotypes and hybrids for West Nile virus is differentially affected by temperature, Parasit. Vectors 9 (2016) 393, https://doi.org/10.1186/s13071-016-1677-0.
[41] W.K. Reisen, Y. Fang, V.M. Martinez, Effects of temperature on the transmission of west nile virus by Culex tarsalis (Diptera: Culicidae), J. Med. Entomol. 43 (2006)

309–317, https://doi.org/10.1603/0022-2585(2006)043[0309:EOTOTT]2.0.CO;2.
[42] A.T. Ciota, A.C. Matacchiero, A.M. Kilpatrick, L.D. Kramer, The Effect of Temperature on Life History Traits of Culex Mosquitoes, J. Med. Entomol. 51 (2014) 55–62, https://doi.org/10.1603/ME13003.
[43] M. Ferraguti, J. Martínez-de la Puente, D. Roiz, S. Ruiz, R. Soriguer, J. Figuerola, Effects of landscape anthropization on mosquito community composition and abundance, Sci. Rep. 6 (2016) 29002, https://doi.org/10.1038/srep29002.
[44] R.R. Montgomery, Age-related alterations in immune responses to West Nile virus infection, Clin. Exp. Immunol. 187 (2017) 26–34, https://doi.org/10.1111/cei.12863.
[45] A.J. Trájer, Meteorological conditions associated with west nile fever incidences in mediterranean and continental climates in Europe, Idojaras. 121 (2017) 303–328.
[46] J. Beauté, G. Spiteri, E. Warns-Petit, H. Zeller, Tick-borne encephalitis in Europe, 2012 to 2016, Eurosurveillance. 23 (2018) 1800201, https://doi.org/10.2807/1560-7917.ES.2018.23.45.1800201.
[47] R.A. Norman, A.J. Worton, L. Gilbert, Past and future perspectives on mathematical models of tick-borne pathogens, Parasitology. 143 (2016) 850–859, https://doi.org/10.1017/S0031182015001523.
[48] F. Roesch, A. Fajardo, G. Moratorio, M. Vignuzzi, Usutu virus: an arbovirus on the rise, Viruses. 11 (2019) 640, https://doi.org/10.3390/v11070640.